

Inactive C8A-humanin analog is as stable as a potent S14G-humanin analog

TSUTOMU ARAKAWA¹, TAKAKO NIIKURA² and YOSHIKO KITA³

¹Alliance Protein Laboratories Inc., San Diego, CA 92121-4746, USA; ²Simon Fraser University, Burnaby, BC V5A 1S6, Canada; ³Department of Pharmacology, Keio University School of Medicine, Tokyo 160-8582, Japan

Received June 6, 2013; Accepted November 12, 2013

DOI: 10.3892/mmr.2013.1797

Abstract. We have previously shown that the structural stability of humanin (HN), a neuroprotective peptide ligand, is one of the attributes to the observed activity differences between HN analogs. It has been observed that the activity increased consecutively in the S7A-HN analog, the parent HN and the S14G-HN analog, consistent with the increased stability observed in that order. In the present study, the structure and stability of another inactive analog, C8A-HN, was measured, which has been revealed to have no neuroprotective activity similar to that of the S7A-HN analog and hence may have compromised stability. While all these analogs of HN demonstrated a similar disordered secondary structure in phosphate-buffered saline at 5°C, as determined by circular dichroism spectroscopy, they revealed different structures at 37°C. At 37°C, less active HN and inactive S7A-HN revealed a structure with a valley at ~217 nm, indicating a conversion from the disordered structure to a β -sheet. Such a conversion was largely irreversible. By contrast, C8A-HN and S14G-HN demonstrated a similar structure at 37°C and at 5°C and remained largely disordered. The observed small structural changes of the C8A-HN analog at 37°C and its reversibility upon cooling do not support a hypothesis that the instability at 37°C may have caused the reduced activity of this analog. Therefore an alternative explanation for its activity loss is required.

Introduction

Short peptides are forming an increasingly significant portion of the biopharmaceutical market (1-4). Humanin (HN) was first identified by the functional screening of genes that protect neuronal cells from apoptotic death caused by a familial

Alzheimer's disease (AD)-linked mutant amyloid precursor protein (5). A gene coding for HN was identified in a cDNA library derived from the occipital lobe of a brain from a patient with AD (5). HN is a 24-amino acid residue peptide (MAPRGFSCLLLLTSEIDLKPKRRA), whose sequence has characteristics of signal peptides (6). Unexpectedly, the endogenous HN produced by the cells transfected with its cDNA-containing plasmid has not only been identified to be partitioned into the cell membrane, but also secreted into the culture media, indicating that the mechanism via which HN acts is that of an extracellular ligand, although its intracellular function cannot be excluded (5,6). The secreted and synthetic HN peptides have shown neuroprotective activities against various toxic stresses (5-8). Synthetic HN was demonstrated to protect neurons from cell death caused by familial AD-linked mutant proteins in neuronal cell lines (5,7,8) and by amyloid- β peptides in mouse cortical primary neurons (5,8-10).

Alanine scanning analysis has revealed several inactive analogs, including S7A-HN and C8A-HN (10). It has been demonstrated that this cysteine at amino acid position eight is in the free SH form and hence is not involved in a disulfide bond (11). The binding of zinc ions to HN through C8 has been indicated to be important in neuroprotection (11). An artificial HN dimer was created by interchain disulfide bond formation, which resulted in reduced activity, meaning that disulfide-linked dimer formation was not the mechanism behind the action of HN and that the artificial dimer may present the functional structure, although with reduced affinity (8). We have previously shown that the strong tendency of S7A-HN to irreversibly change its conformation and aggregate under physiological conditions may be, at least in part, responsible for the observed loss of its neuroprotective activity (12,13). Such aggregation would obscure the results of the biological activity of C8A-HN and possibly other HN analogs, and hence, in the present study, the structure of this analog in comparison with HN and other HN analogs was characterized.

Materials and methods

Peptide analog preparation. HN, S7A-HN and S14G-HN were obtained from Peptide Institute, Inc. (Osaka, Japan) and C8A-HN was purchased from KNC Laboratories Co., Ltd. (Kobe, Japan). The purity was confirmed to be at least 95% by the vendor using an amino acid and liquid

Correspondence to: Dr Tsutomu Arakawa, Alliance Protein Laboratories, 6042 Cornerstone Court West, Suite A, San Diego, CA 92121-4746, USA
E-mail: tarakawa2@aol.com

Key words: humanin, inactive analog, circular dichroism, disordered structure, aggregation

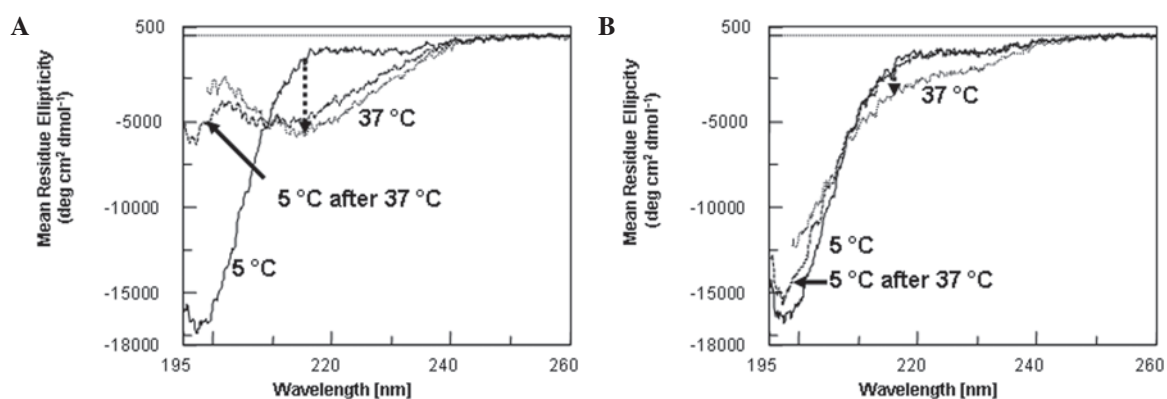


Figure 1. Far-UV CD spectra of (A) HN and (B) S14G-HN. Solid, dotted and dashed curves correspond to the spectra at 5, 37 and 5°C after heating to 37°C, respectively. The 37°C spectrum was recorded after incubating the sample at 37°C for 15 min. Following the 37°C measurement, the sample was cooled to 5°C and incubated at 5°C for 15 min. The dashed arrow indicates the change at 217 nm due to a temperature shift from 5 to 37°C. UV, ultraviolet; CD, circular dichroism; HN, humanin.

chromatography-mass spectrometry analysis. These peptides were dissolved at 1 mg/ml in cold water and kept cold until use. Phosphate-buffered saline (PBS; 1.1X) was prepared from 10X PBS and also kept cold until use. The peptide solution in cold water was diluted with the cold 1.1X PBS to a final concentration of 0.1 mg/ml and 1X PBS. The diluted solution was immediately delivered to the circular dichroism (CD) cell and placed in the Peltier cell holder set at 5°C. CD spectral or time-course measurements were then acquired as described in the results section.

CD spectroscopy measurements. CD measurements were recorded on a Jasco J-715 spectropolarimeter (Jasco Inc., Easton, MD, USA) at the indicated temperatures using a 0.1-cm cell throughout with the following parameters: A 10-nm/min scan rate, five accumulations, a 0.1-nm data pitch and a 4-sec time constant. The sample temperature was controlled with a Peltier cell holder (Jasco Inc.) and a PTC-348WI temperature controller (Jasco Inc.). The CD spectra were converted to the mean residue ellipticity following subtraction of the PBS spectrum using the peptide concentration (0.1 mg/ml), the mean residue weight (112 g/mol for HN, S7A-HN and C8A-HN and 111 g/mol for S14G-HN) and the pathlength of the cell (0.1 cm).

Results and Discussion

Far-ultraviolet (UV) CD spectra of HN were determined as a function of temperature, *i.e.*, at 5, 37 and then 5°C again following the 37°C measurements (Fig. 1A). The spectrum at 5°C (solid curve) was essentially identical to the previous data and was characterized as primarily disordered (1). The cell temperature was then raised to 37°C and the sample was kept at 37°C for 15 min. The spectrum at 37°C was entirely different from the 5°C spectrum, with a valley around 217 nm (dotted curve). The change at 217 nm is indicated by an arrow in Fig. 1A. The spectrum is characteristic of the β -sheet structure that may be observed in antibody structures (14), most likely due to the aggregation of the peptide, leading to intermolecular β -sheet formation. We have previously shown using a sedimentation velocity technique that the HN and HN analog extensively aggregate into different sizes in PBS at 25°C (13).

Following the 37°C measurement, the sample temperature was cooled to 5°C and then maintained at 5°C for 15 min. The cooled sample (Fig. 1, dashed curve) demonstrated no recovery of the original spectrum, largely retaining the shape of the 37°C spectrum. Such a spectrum is consistent with the irreversible nature of structural change at 37°C due to aggregation. A similar result was obtained for S7A-HN (data not shown): Namely, the disordered structure at 5°C was converted to the spectrum characteristic of the interpeptide β -sheet at 37°C and was not recovered upon cooling. This analog also revealed extensive aggregation, as determined by the sedimentation velocity technique (13).

By contrast, the results for S14G-HN and C8A-HN were qualitatively different from the aforementioned two samples. The far-UV CD spectra of S14G-HN were determined at 5°C (solid curve), 37°C (dotted curve) and 5°C subsequent to heating (dashed curve) (Fig. 1B). It is evident that these three spectra were not much different from each other. The spectrum at 5°C was similar to the 5°C spectrum for HN (Fig. 1A), *i.e.*, that of a disordered structure. There were only small changes upon heating to 37°C (as indicated by a small arrow at 217 nm). The spectrum at 37°C showed the structure to have remained largely disordered, without the appearance of a 217 nm valley, and was almost restored upon cooling; namely, the small changes induced by heating to 37°C were largely reversible. A similar conclusion may be made for C8A-HN (data not shown). In the case of C8A-HN, the original 5°C spectrum was completely restored upon cooling.

The differences in reversibility between these peptides appear to be ascribed to the structure at 37°C. The far-UV CD spectra at 37°C were compared among these four peptides (Fig. 2). The spectra of HN (dotted curve, also shown by the arrow) and S7A-HN (dashed curve) have a valley, although at different wavelengths, indicating that they undergo a transition into β -sheet aggregates. It appears that the analogs have marginally different secondary structures. Conversely, the spectra of S14G-HN (solid curve) and C8A-HN (double dashed curve) are similarly disordered, indicating that these HN analogs have an identical secondary structure at 37°C. This indicates that S14G-HN and C8A-HN have less or no tendency to form β -sheet aggregates upon heating, although a

Table I. CD signal change due to a temperature shift.

Sample	Change at 201 nm, mdeg		Recovery, % (n/total n)
	5→37°C	37→5°C	
HN	10	2	20 (2/10)
S7A-HN	8	2	25 (2/8)
S14G-HN	2	2	100 (2/2)
C8A-HN	2	2	100 (2/2)

HN, humanin; CD, circular dichroism.

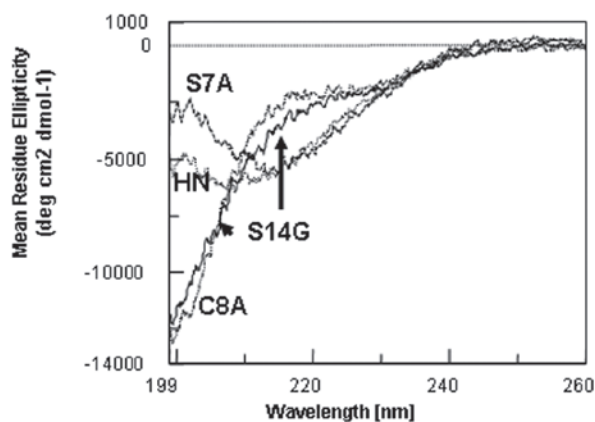


Figure 2. Far UV-CD spectra of HN and HN analogs at 37°C. Solid and double-dashed curves correspond to the spectra for S14G-HN and C8A-HN. Dotted and dashed curves correspond to the spectra for HN and S7A-HN. UV, ultraviolet; HN, humanin; CD, circular dichroism.

sedimentation analysis of C8A-HN has not yet been performed. This explains why the structural changes are reversible upon heating, i.e., the lack of aggregation. Such aggregation for HN and S7A-HN occurs only at 37°C, as all these HN forms are similar and largely disordered at 5°C (data not shown).

The time-course of heat-induced structural changes and their reversibility were examined as follows. Previously, we have used a wavelength at 201 nm to follow the time-course, as the change in CD intensity is greatest at this wavelength (12). However, it does not correspond to a change in specific secondary structures, e.g., an α -helix or β -sheet. As observed in Fig. 1, the signal at 217 nm significantly changed upon heating and corresponded to an induction of a β -sheet structure for HN and S7A-HN (see arrow for the changes in the CD signal). However, this wavelength was not informative for S14G-HN and C8A-HN, as observed in Fig. 1B (smaller arrow). The changes at 217 nm were too small to follow the structural changes for S14G-HN and C8A-HN. The time-course of signal changes at 201 nm upon heating was determined for HN (Fig. 3). In Fig. 3A, the sample temperature was raised from 5 to 37°C at time zero. It took ~120 sec to bring the temperature to 37°C, as indicated by the black bar. There were slow increases in the CD intensity, consistent with the spectral changes observed in Fig. 1. The signals appeared to reach a plateau around 1,000 sec. Following completion of a 20-min time-course measurement, the sample temperature

was immediately dropped to 5°C and then the CD signal at 201 nm was followed in Fig. 3B. The signal at time zero was close to the signal at 1,200 sec (Fig. 3A), meaning that the structure at 37°C remained intact immediately after changing the temperature to 5°C. There were only small decreases in the 201-nm intensity with a 5°C incubation, the final value at 1,200 sec being far from the value of -13 mdeg for the starting structure (prior to heating to 37°C). The results were consistent with the spectral changes in Fig. 1A. The changes in CD intensity upon the temperature shift are summarized in Table I. It is evident that the structural changes caused by heating at 37°C are largely irreversible for HN.

The same results were replotted in Fig. 4A for HN; changes due to a temperature increase (solid curve, 5→37°C) and subsequent decrease (dotted curve, 37→5°C) are plotted on the same panel. Fig. 4B shows the results for S7A-HN. The signal change upon heating was marginally smaller for S7A-HN than HN. However, these peptides were similar in reversibility. The signal changes induced by heating at 37°C were irreversible upon cooling. Additionally, it is evident that these two peptides were marginally different with regard to the time-course. The 201-nm signal change appeared to occur faster for S7A-HN than for HN (when comparing Fig. 4A and B). If, in fact, this signal change was due to aggregation, the result indicates that S7A-HN aggregates faster upon incubation at 37°C.

The changes at 201 nm upon heating and cooling for S14G-HN and C8A-HN were also determined as a function of incubation time (data not shown). For S14G-HN and C8A-HN, the 201 nm signal changed marginally upon heating to 37°C and was fully recovered upon cooling. For S14G-HN and C8A-HN, the signal changes were much smaller than HN and S7A-HN (Table I), ~20-25% those for HN and S7A-HN. As demonstrated by the changes upon cooling (Table I), the recovery of the CD signal was ~100%, indicating an apparent full reversibility. Such reversibility is consistent with the theory that S14G-HN and C8A-HN do not aggregate upon heating at 37°C under the experimental conditions. The time-course of signal change upon heating appears to be identical for S14G-HN and C8A-HN (data not shown). Thus, it may be concluded that there is no difference between S14G-HN and C8A-HN in terms of the stability at 37°C.

The present study also analyzed how the temperature-dependent structural changes and aggregation affect the biological activity of the HN and HN analogs. We have previously suggested the possibility that the instability of S7A-HN at 37°C is at least one of the factors responsible for the observed lack of biological activity (12); namely, that it may aggregate in a physiological solution prior to reaching its target site during *in vitro* or *in vivo* assays. Thus, those peptides that have a greater tendency to aggregate at 37°C may lose activity. In the present study, the inactive C8A-HN behaved differently from the inactive S7A-HN and was similar to the potent S14G-HN analog, meaning that the stability at 37°C did not correlate with the loss of neuroprotective activity for C8A-HN. One possibility is that C8A-HN in fact lost its ability to bind to the target site to which the active HN and S14G-HN bind. However, it should be noted that the S14G-HN that revealed no apparent aggregation tendency in the present study does aggregate under harsher conditions, e.g., prolonged incubation, higher

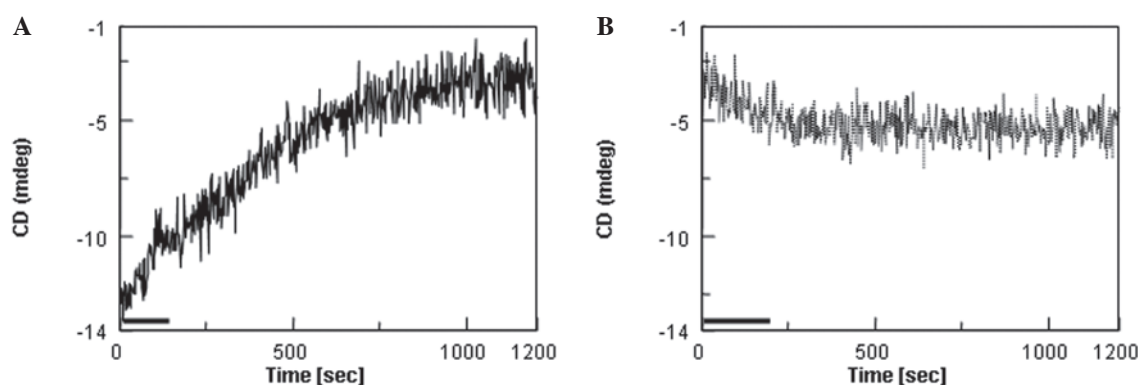


Figure 3. Time-course of CD signal change at 201 nm for HN upon temperature shift from (A) 5 to 37 °C and (B) 37 to 5°C. (A) The sample temperature was changed from 5 to 37 °C at time zero. It took ~120 sec to reach 37°C (shown by a bar). (B). After reaching 1,200 sec in (A), the sample temperature was immediately shifted from 37 to 5°C at time zero. It took ~200 sec to reach 5°C (shown by a bar). CD, circular dichroism; HN, humanin.

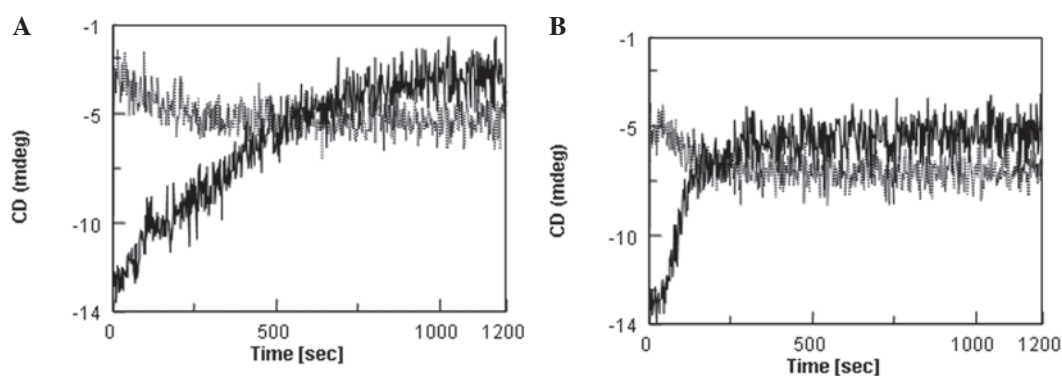


Figure 4. Time-course of CD signal change at 201 nm for (A) HN and (B) S7A-HN. The solid curve corresponds to the 201 nm signal change due to temperature shift from 5 to 37°C. The dotted curve corresponds to the 201 nm signal change due to a temperature shift from 37 to 5°C. CD, circular dichroism; HN, humanin.

temperature, higher peptide concentration and higher ionic strength (13,15-17). Thus, it is possible that C8A-HN aggregates under certain bioassay conditions, resulting in activity loss. In other words, this analog may be active depending on the bioassay system that is capable of reducing exposure to harsh conditions and thereby minimize aggregation. In fact, the preliminary bioassay results of C8A-HN, based on phosphorylation of early response kinase stimulated by the HN peptides through their receptor, indicated C8A-HN to be active (Kita and Niikura, unpublished data).

In the present study, an attempt was made to relate the effects of these mutations on HN aggregation to the physical properties of the side chain of each mutated amino acid. Since HN is disordered, it is more likely that these amino acid side chains are solvent-exposed. The solvent-exposed sequence may be analyzed by a computer program to predict the aggregation or fibrillation tendency. In the present study, the Waltz program was used (18). Using the highest sensitivity for the propensity of aggregation, the following sequences were shown to be prone to aggregation: S7-I16 for HN, F6-I16 for S7A-HN, G5-I16 for C8A-HN and S7-G14 for S14G-HN. The observed aggregation of HN, S7A-HN and S14G-HN appears to agree with the prediction that a greater tendency for aggregation correlates with the longer predicted sequence. However, the observed deviation for C8A-HN (the longest sequence) requires further explanation.

As expected, all these sequences contain L9-L12, indicating that the hydrophobicity is also involved in the observed aggregation. Side chain hydrophobicity has been determined by a pioneering study by Nozaki and Tanford (19). The free energy of the transfer of the glycine side chain from ethanol (i.e., core environments of the folded protein structure or aggregated structure) to water was assumed to be zero; in other words, the glycine side chain has no preference for water over hydrophobic environments. A serine side chain is more stable in water than a glycine side chain by a transfer free energy of -300 cal/mol, meaning that a S14G mutation should render S14G-HN less polar or more hydrophobic, as this mutation loses favorable interaction free energy of the serine side chain with water. This disagrees with the lower observed aggregation tendency of S14G-HN or the Waltz prediction. This may be explained by the unique structural nature of glycine, as pointed out by Richardson and Richardson (20); glycine is well known to form a local structure around glycine making it more mobile, facilitating backbone motion and favoring the disordered structure. While the S14G mutation renders S14G-HN less polar, it may stabilize the disordered structure and prevent conversion into a more folded β -sheet, and thereby into an aggregated structure. This may be why the Waltz prediction demonstrated termination at residue G14 in the present study. With regard to S7A-HN, the alanine side chain is non-polar by 500 cal/mol, i.e., its side chain interaction with

water is highly unfavorable. Combining the polar nature of the serine side chain and the non-polar nature of the alanine side chain, the S7A mutation renders S7A-HN highly hydrophobic, consistent with a one amino acid excess over the parental HN in the Waltz prediction. No free energy of transfer data is available for the cysteine side chain. Using the hydropathy scale of Kyte and Doolittle (21) shows, however, that a cysteine side chain is more hydrophobic than an alanine side chain, meaning that the C8A mutation reduces the hydrophobicity, consistent with its weaker aggregation, although inconsistent with the Waltz prediction.

A number of short peptides behave similarly to HN, i.e., they are largely disordered in aqueous solutions and have the tendency to aggregate, often leading to structures termed β -amyloid fibrils (22-26). Peptides are clinically significant biopharmaceuticals (1-4) and their development requires stable formulations, physically and chemically, for long-term storage. Considering the irreversible nature of aggregation, as observed in the present study for HN, there is a requirement to design a formulation of short peptides in order to minimize aggregation.

In conclusion, less active HN and inactive S7A-HN demonstrated larger and irreversible structural changes upon heating than the more active S14G-HN analog. Notably, the C8A-HN analog, which has been previously reported to be inactive, revealed a weak aggregation tendency similar to S14G-HN, indicating that the activity of C8A-HN may be compromised due to factors other than instability under physiological conditions.

References

- Fields K, Falla TJ, Rodan K and Bush L: Bioactive peptides: signaling the future. *J Cosmet Dermatol* 8: 8-13, 2009.
- Aneiros A and Garateix A: Bioactive peptides from marine sources: pharmacological properties and isolation procedures. *J Chromatogr B Analyt Technol Biomed Life Sci* 803: 41-53, 2004.
- Mason JM: Design and development of peptides and peptide mimetics as antagonists for therapeutic intervention. *Future Med Chem* 2: 1813-1822, 2010.
- Otvos L Jr: Synthesis of a multivalent, multiepitope vaccine construct. *Methods Mol Biol* 494: 263-273, 2008.
- Hashimoto Y, Niikura T, Tajima H, *et al*: A rescue factor abolishing neuronal cell death by a wide spectrum of familial Alzheimer's disease genes and Abeta. *Proc Natl Acad Sci USA* 98: 6336-6341, 2001.
- Yamagishi Y, Hashimoto Y, Niikura T and Nishimoto I: Identification of essential amino acids in Humanin, a neuroprotective factor against Alzheimer's disease-relevant insults. *Peptides* 24: 585-595, 2003.
- Hashimoto Y, Kurita M and Matsuoka M: Identification of soluble WSX-1 not as a dominant-negative but as an alternative functional subunit of a receptor for an anti-Alzheimer's disease rescue factor Humanin. *Biochem Biophys Res Commun* 389: 95-99, 2009.
- Hashimoto Y, Niikura T, Ito Y, *et al*: Detailed characterization of neuroprotection by a rescue factor humanin against various Alzheimer's disease-relevant insults. *J Neurosci* 21: 9235-9245, 2001.
- Ikonen M, Liu B, Hashimoto Y, *et al*: Interaction between the Alzheimer's survival peptide humanin and insulin-like growth factor-binding protein 3 regulates cell survival and apoptosis. *Proc Natl Acad Sci USA* 100: 13042-13047, 2003.
- Terashita K, Hashimoto Y, Niikura T, *et al*: Two serine residues distinctly regulate the rescue function of Humanin, an inhibiting factor of Alzheimer's disease-related neurotoxicity: functional potentiation by isomerization and dimerization. *J Neurochem* 85: 1521-1538, 2003.
- Armas A, Sonois V, Mothes E, Mazarguil H and Faller P: Zinc(II) binds to the neuroprotective peptide humanin. *J Inorg Biochem* 100: 1672-1678, 2006.
- Arakawa T, Niikura T and Kita Y: The biological activity of Humanin analogs correlates with structure stabilities in solution. *Int J Biol Macromol* 49: 93-97, 2011.
- Arisaka F, Arakawa T, Niikura T and Kita Y: Active form of neuroprotective Humanin, HN, and inactive analog, S7A-HN, are monomeric and disordered in aqueous phosphate solution at pH 6.0; No correlation of solution structure with activity. *Protein Pept Lett* 16: 132-137, 2009.
- Thies MJ, Talamo F, Mayer M, *et al*: Folding and oxidation of the antibody domain C(H)3. *J Mol Biol* 319: 1267-1277, 2002.
- Arakawa T, Niikura T, Tajima H and Kita Y: The secondary structure analysis of a potent Ser14Gly analog of antiAlzheimer peptide, Humanin, by circular dichroism. *J Pept Sci* 12: 639-642, 2006.
- Arakawa T, Kita Y and Niikura T: A rescue factor for Alzheimer's diseases: discovery, activity, structure, and mechanism. *Curr Med Chem* 15: 2086-2098, 2008.
- Pistolesi S, Rossini L, Ferro E, Basosi R, Trabalzini L and Pogni R: Humanin structural versatility and interaction with model cerebral cortex membranes. *Biochemistry* 48: 5026-5033, 2009.
- Maurer-Stroh S, Debulpaep M, Kuemmerer N, *et al*: Exploring the sequence determinants of amyloid structure using position-specific scoring matrices. *Nature Methods* 7: 237-242, 2010.
- Nozaki Y and Tanford C: The solubility of amino acids and two glycine peptides in aqueous ethanol and dioxane solutions. Establishment of a hydrophobicity scale. *J Biol Chem* 246: 2211-2217, 1971.
- Richardson JS and Richardson DC, Principles and patterns of protein conformation. In: *Prediction of Protein Structure and the Principles of Protein Conformation*. Fasman G (ed). Plenum Press, New York, pp43-75, 1989.
- Kyte J and Doolittle RF: A simple method for displaying the hydropathic character of a protein. *J Mol Biol* 157: 105-132, 1982.
- Zhou X, Liu J, Li B, Pillai S, Lin D, Liu J and Zhang Y: Assembly of glucagon (proto)fibrils by longitudinal addition of oligomers. *Nanoscale* 3: 3049-3051, 2011.
- Arvinte T, Cudd A and Drake AF: The structure and mechanism of formation of human calcitonin fibrils. *J Biol Chem* 268: 6415-6422, 1993.
- Steckmann T, Awan Z, Gerstman BS and Chapagain PP: Kinetics of peptide secondary structure conversion during amyloid β -protein fibrillogenesis. *J Theor Biol* 301: 95-102, 2012.
- Kodali R, Williams AD, Chemuru S and Wetzel R: Abeta(1-40) forms five distinct amyloid structures whose beta-sheet contents and fibril stabilities are correlated. *J Mol Biol* 401: 503-517, 2010.
- Macchi F, Hoffmann SV, Carlsen M, *et al*: Mechanical stress affects glucagon fibrillation kinetics and fibril structure. *Langmuir* 27: 12539-12549, 2011.